Desalination and Water Treatment
www.deswater.com
doi: 10.1080/19443994.2014.981863

57 (2016) 1949–1958
January

Taylor & Francis
Taylor & Francis Group

Zeolite-induced catalytic ozonation of p-aminobenzenesulfonic acid in a bubbling reactor

S. Zhang[a,b,*], D. Wang[c], P.P. Fan[a,b], L. Zhou[d]

[a]*School of Environmental and Municipal Engineering, Tianjin Chengjian University, Jinjing Road 26, Tianjin 300384, China, Tel. +86 13820306663; email: zssci1203@163.com (S. Zhang), Tel. +86 13820196660; email: 13820196660@163.com (P.P. Fan)*
[b]*Tianjin Key Laboratory of Aquatic Science and Technology, Tianjin 300384, China*
[c]*Key Laboratory of Industrial Ecology and Environmental Engineering (MOE), School of Environmental Science and Technology, Dalian University of Technology, Linggong Road 2, Dalian 116024, China, Tel. +86 13940950507; email: wangdong@dlut.edu.cn*
[d]*East China Engineering Science and Technology Co. Ltd., Wangjiang East Road 70, Hefei 230000, China, Tel. +86 18355127631; email: 455108578@qq.com*

Received 2 April 2014; Accepted 23 October 2014

ABSTRACT

This work investigated the effect of zeolite on ozonation of p-aminobenzenesulfonic acid (PAA) as model compound. Four H^+-form ZSM-5 samples (labeled as HZSM-5) with respective silica/aluminum molar ratio of 25, 50, 80, and 360 were employed for comparative study and characterized before use in terms of framework structure, crystallinity, texture, surface acidity, and morphology. In ozonation process dealing with PAA, there was no remarkable impact of HZSM-5 at pH 3.5, while for scenarios of pH 9.5, the decay rate of target contaminant largely accelerated with addition of HZSM-5 zeolite acting mainly as ozone catalyst. It was interesting to note that HZSM-5 (25) compared to other zeolite congeners performed to be more effective in catalytic ozonation for degradation and mineralization of PAA. Process analysis suggested that the weak Lewis acid sites on zeolite surface might have played major role in facilitating the consumption of hydroxyl groups (Al–OH or Si–OH) and anions (OH^-) by molecular ozone, expediting locally the progress of $HO^{\cdot}$ generation and depletion giving rise to advanced oxidation. Leaching of aluminum ion during ozonation was monitored, and results indicated that elevation of pH, in favor of zeolite-induced catalysis, could appreciably inhibit de-aluminum coupled to material stability.

Keywords: ZSM-5 zeolite; Characterization; Ozonation; Surface acidity; Catalysis

1. Introduction

Bubbling ozone treatment is a promising alternative oxidation method dealing with water and wastewater [1–3]. Molecular ozone can break up aromatic compounds with nucleophilic positions [4] or unsaturated aliphatics [5], whereas it cannot accomplish deep oxidation for the selectivity and low power ($E^0(O_3/H_2O$ = 2.07 V). Highly oxidative hydroxyl radical ($HO^{\cdot}$) can be produced as a result of ozone hydrolysis, allowing the occurrence of advanced oxidation processes (AOPs) capable to disrupt or even mineralize organic contaminants ($E^0(HO/H_2O$ = 2.80 V). However, the $HO^{\cdot}$-induced pathway by plain ozonation normally

*Corresponding author.

presents to be rather weak unless solution pH was adjusted higher than 10 as suggested by Beltrán et al. [6], because an ample amount of HO• can not be produced owing to the finite transformation rate of aqueous O_3 into HO• species consuming mainly hydroxyl anions [7]. On the other hand, the short-lived HO• is susceptible to be quenched once generated in liquid bulk, which is usually caused by ozonation products such as carbon dioxide in inorganic form of carbonate or bicarbonate [8]. A feasible resolution to intensify the production of HO• and/or its effective utilization for AOPs is to develop heterogeneous ozonation by virtue of functionalized solid species. This is because the presence of some solid phase can potentially exert chemical impact, including adsorptive removal of organic loading as molecular sieve, concentration of oxidant and target molecules as process accelerator [9], effective transformation of molecular ozone into (HO•) as catalyst [10], and enhancement of gas–liquid mass transfer as promoter [11].

Zeolite is aluminosilicates in crystal framework structures containing cavities that are occupied by large ions and water molecules. It can be naturally exploited or artificially synthesized with good mechanical/hydrothermal stability as well as regular porosity. Quite recently, zeolite began to be introduced environmentally as low-cost catalyst in combination with ozone [12–19]. The surface chemistry of zeolite is recognized to be of paramount importance in heterogeneous catalysis, which is mainly subject to HO-groups (Brønsted acid centre), aluminum-containing extra-framework species (Lewis sites), and alkaline metal contributed cations (or basic sites). Valdés et al. [13] reported that acid-modified zeolite could be effective catalyst for ozonation of toxic organics, and they suggested the hydrous groups present on metal surface oxides of zeolite play a fundamental role. Ikhlaq et al. [15] reported that aluminum content of zeolite could promote the formation of superoxide ion radicals (O_2^-) that in turn facilitates the production of HO• consuming ozone. Yet the performance of zeolite on ozonation process is still not a matter of consensus. Rivera-Utrilla et al. [16] indicated that the surface acid sites of zeolite principally stabilize O_3 molecules and in turn play negative role on ozonolysis to produce (HO•). Amin et al. [17] concluded that zeolite-ozone system exhibited screening effect for removal of phenol and COD mainly by adsorption rather than catalytic process, for which the surface of zeolite could only contribute to the interaction of molecular ozone and organics.

Besides the effect of material surface chemistry, solution pH is commonly an influential factor that may even affect the process of heterogeneous catalytic ozonation. This is because the pH environment may chemically alter the surface acid–base property which closely correlates with the process of catalysis, locally giving rise to a synergistic effect facilitating or accelerating the generation of HO• [20,21]. Concerning zeolite-induced catalytic ozonation, moreover, it is still in argument where the reactions between HO• species formed by catalysis and organic compound principally take place, since either in liquid bulk phase [22] or the surface region of zeolite [14] has been documented by researchers. In addition to the power of catalysis, material stability should be evaluated for utilization of zeolite as the leaching of aluminum content could inevitably occur during reactions, and this undesired issue in application of zeolite may have significant implications with the pH environment. In view of the relevant works completed, therefore, efforts still need to be made for collection of information with guiding significance for development of zeolite-ozone multiphase systems.

The surface property of zeolite largely depends on the proportional silica (Si) to aluminum (Al) arrangement in framework and extra-framework structures [23]. In this study, four ZSM-5 samples, with respective Si/Al molar ratio of 25, 50, 80, and 360, were comparatively characterized and experimented for catalytic ozonation of p-aminobenzenesulfonic acid (PAA) as model compound, where the catalytic role played by zeolite during ozonation process was analyzed and discussed.

2. Experimental

2.1. Materials

Granular ZSM-5 zeolites with respective Si/Al molar ratio of 25, 50, 80, and 360 were purchased from Catalyst Plant of Nankai University (Tianjin, China). Prior to use, they were rinsed with boiled distilled water until the pH reached a constant level, dried at 100°C for 12 h, and then calcinated at 550°C for 4 h in muffle furnace to decompose the NH_3-form and remove the organic impurities [24]. Then, H^+-form ZSM-5 samples were produced labeled as "HZSM-5". The PAA was supplied by Damao Reagent (Tianjin, China) and employed as the model contaminant.

2.2. Ozonation and catalytic ozonation

Experiments were carried out in a batch mode Plexiglas cylindrical column with 0.1 m internal diameter (see Fig. 1). Ozone mixed gas (containing mainly O_3, O_2, and N_2) was bubbling introduced at the bottom of reactor at 3 L min^{-1} with inlet gaseous

ozone concentration of 25 g Nm^{-3}. The initial PAA concentration of 60 mg L^{-1} was preset in 1.5 L ultrapure water for each experiment, and the liquid temperature was controlled at 20 ± 0.5℃ by a thermostat (Scientz Biotechnology Co. Ltd., Ningbo, China). Solid loading of zeolite particles was kept at 5 g L^{-1} for catalytic ozonation tests. Solution pH was initially adjusted by adding 0.1 M hydrochloric acid or 0.1 M sodium hydroxide solutions and maintained during reactions by means of dropwise regulation. All the reactions were completed under atmospheric pressure condition.

2.3. Analysis methods

Fourier transform infrared (FT-IR) spectra were recorded between 1,400 and 400 cm^{-1} with Bruker Vector FT-IR spectrometer (sample amount was about 1 wt.%; pure potassium bromide was utilized as reference). X-ray diffraction (XRD) patterns were acquired using DX-3000 X-ray diffractometer (Shimadzu, Japan) with Cu Kα monochromatic radiations and operated at 40 kV and 100 mA. The surface morphology was examined using scanning electron microscopy (SEM) (S4800, Hitachi, Japan). The surface acidity was evaluated by NH_3 temperature-programmed desorption (NH_3-TPD) using CheBET Pulsar TPD Analyzer (Quantachrome, USA). Experimental runs were recorded by heating the samples in N_2 (30 mL min^{-1}) from 100 to 800℃ at a heating rate of 10℃ min^{-1}. Diffuse reflectance (DRIFT) spectra of pyridine adsorbed at 150℃ and 450℃ were obtained with EQUINOX55 (Germany) spectrometer. Textural properties were determined by Autosorb-1 (Quantachrome, USA). The N_2 adsorption/desorption isotherms at about −196.15℃ were measured, and the specific surface area (SSA) was calculated using the Brunauer–Emmett–Teller (BET) model.

Concentration of PAA was detected by HPLC (Waters Alliance HPLC 2695-2996) at wavelength of 250 nm. The stationary phase was Ultimate XB-C18 5 μm column (250 × 4.6 mm) with an eluent solution mixed by A (0.3% acetic acid and 0.3% triethylamine) and B (methanol) under flow rate of 0.8 mL min^{-1} ($V_A/V_B = 90/10$). Total organic carbon (TOC) was measured using TOC-V_{CPH} analyzer (Shimadzu, Japan). Solution pH was measured by digital pH meter (Cyber Scan pH1500). Electron paramagnetic resonance test was conducted for detection of free radicals using Bruker A200 (Germany). The concentration of aluminum ions (i.e. Al^{3+}) was measured by a simultaneous inductively coupled plasma optical emission spectrometer (ICP-OES, Optima 2000 Series, Perkin Elmer, USA) with axial views at wavelength of 396.153 nm.

Gaseous ozone concentration of inlet ($[O_3]_{g,in}$) and outlet ($[O_3]_{g,out}$) was monitored by Portable-BD5Gas2610 Ozone Analyzer (BigDipper Co. Ltd, Beijing, China), and the consumption rate (%) of feeding ozone was calculated by the following equation:

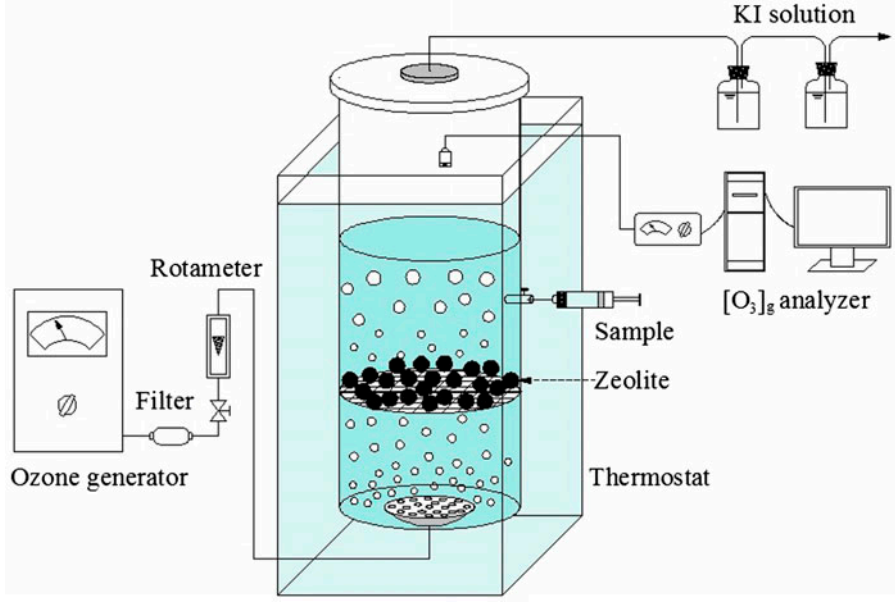

Fig. 1. The schematic diagram of experimental apparatus for zeolite-ozone treatment.

$$\text{Ozone consumption}\ (\%) = \frac{[O_3]_{g,in} - [O_3]_{g,out}}{[O_3]_{g,in}} \times 100\ (\%) \quad (1)$$

3. Results and discussion

3.1. Characterization of zeolite samples

The thermal-treated HZSM-5 zeolites were comparatively characterized in this section. FT-IR spectra are displayed in Fig. 2. There are two frequency groups including internal vibration insensitive to structure and vibration of external linkages between tetrahedral due to topology and the mode of structure arrangement [25]. Peaks at band of 455.2 cm^{-1} and 796.6 cm^{-1} are respectively assigned to the bending and symmetric stretching vibration of internal tetrahedron, while at 1,099.4 cm^{-1} and 1,224.8 cm^{-1} denotes asymmetric stretching vibration of external tetrahedral. Band at 549.7 cm^{-1} may represent a pseudo-lattice or secondary vibration. The vibration intensity of external tetrahedral structure referring to 1,099.4 cm^{-1} and 1,224.8 cm^{-1} decreased with increasing Si/Al molar ratio, suggesting aluminum species is the key node for tetratomic rings in external aluminosilicate framework. The bands due to zeolitic water commonly lie in the range of 1,600–3,700 cm^{-1}. IR band at 1,622.1 cm^{-1} is connected to the deformation vibration of absorbed water molecules and at 3,460.3 cm^{-1} is attributed to vibration of bonds HO–(Si^{4+} or Al^{3+}). The XRD pattern shown by inset of Fig. 2 demonstrates that the HZSM-5 zeolites employed were well crystallized, and data in Table 1 show that they own similar intensity of spectra peaks to starting material. Results of textural properties of HZSM-5 were also recorded in Table 1 where all the zeolites presented quite close in micro-porous structure, pore volumes, and SSAs.

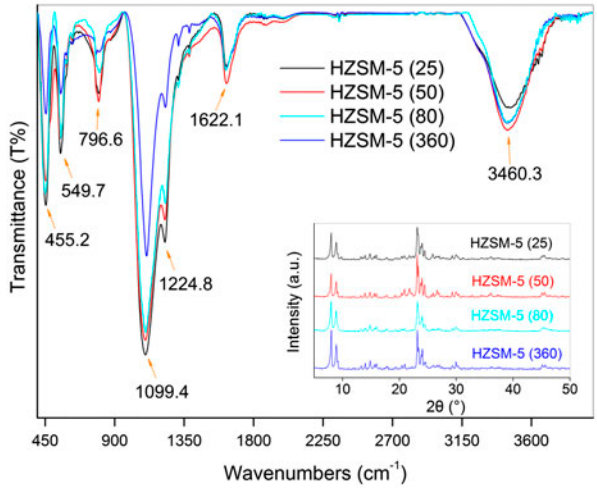

Fig. 2. FT-IR spectra of HZSM-5 zeolites (inset: XRD pattern of HZSM-5 zeolites).

NH_3-TPD was used to characterize the total amount of surface acidity (see Fig. 3). The relative position of the temperature maximum in the plot of the ammonia desorption vs. temperature is an indication of the magnitude of the ammonia desorption activation energy and consequently the relative acid strength of the sites (above 100°C was considered as chemisorbed NH_3). It can be seen in Fig. 3 that the total acidity decreased with increasing Si/Al molar ratio, and HZSM-5 (25) sample exhibited the highest density of acid under whatever desorption temperature.

Infrared spectroscopy of adsorbed pyridine discriminates the nature of the acid sites composed of Brønsted sites and Lewis sites [26]. Pyridine bound to Brønsted acid sites is associated with IR band at 1,545 cm^{-1}, bound to Lewis acid sites is tied to a band at 1,450 cm^{-1}, and at 1,490 cm^{-1} was due to pyridine adsorbed on both Brønsted and Lewis acid sites. As indicated by Fig. 4, the amount of Brønsted acid was generally higher than Lewis acid under whatever temperature (150°C for weak acid and 450°C for strong acid sites). The calculated ratio of Lewis and Brønsted acid amount was presented in Table 1. One can see that HZSM-5 (50) sample compared to others exhibited to own a relative higher amount of Brønsted sites (remarkably lower in values of L^*/B^*), suggesting that much more aluminum atoms for HZSM-5 (50) are in protonated tetrahedral structures rather than a state of trivalent coordination linked to Lewis acid sites [23].

Surface morphology of HZSM-5 was examined by SEM, and images are shown in Fig. 5. Numerous micro-clusters accumulated forming blocky and layered structure that seemed like a fragmentation of surface. HZSM-5 (50) sample with higher amount of Brønsted acid presented to be somewhat smoother and more compact compared to others (see Fig. 5(b)), which might be explained by that the tetrahedral aluminum (associated with H^+) accounting for Brønsted acidity is in relative rich amount and well-isolated in skeleton of zeolite.

3.2. Catalytic ozonation of PAA

Fig. 6 shows the evolution of normalized PAA concentration during ozonation with or without HZSM-5 particles. The rate for plain ozonation of PAA at pH 3.5 presented to be much slower than that obtained at

Table 1
Relevant properties of ZSM-5 zeolites used in this work ("S" and "P" represent respectively the starting material and that underwent thermal pretreatment)

	SSA ($m^2\ g^{-1}$)		Pore volume ($cm^3\ g^{-1}$)		Average pore size (nm)			L^*/B^{*b} (−)	
Si/Al (−)	S	P	S	P	S	P	Crystallinity[a] (%)	150°C	450°C
25	276.26	307.75	0.263	0.309	3.81	4.01	88.8	0.730	0.663
50	275.19	248.47	0.265	0.239	3.85	3.85	94.9	0.257	0.159
80	291.17	264.20	0.356	0.360	4.89	5.44	98.8	1.197	0.910
360	281.95	287.78	0.288	0.287	4.08	3.99	98.5	0.812	0.314

[a]Crystallinity was measured by determining the intensities of the main X-ray diffraction peaks. The starting material was assumed to be 100%.
[b]The amount ratio of Lewis and brønsted acid sites were calculated by integration of absorbance signal at band 1,450 cm^{-1} and 1,545 cm^{-1}.

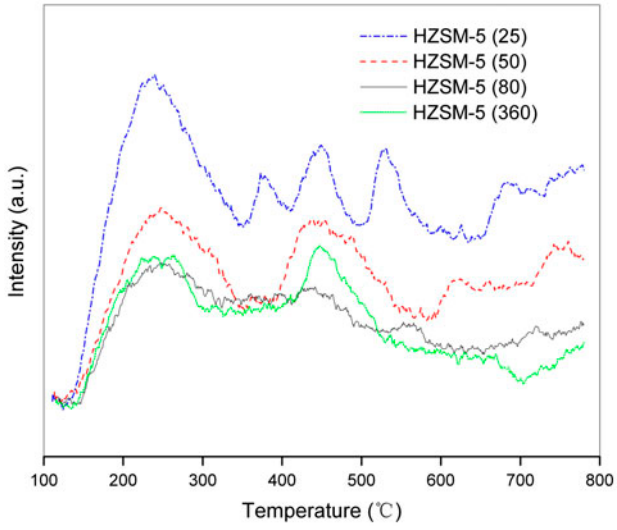

Fig. 3. Profiles of NH_3-TPD from HZSM-5 zeolites (condition: heating rate of 10°C min^{-1} under N_2 flow at 30 mL min^{-1}).

pH 9.5, because acidic solution in lack of hydroxyl anion (OH^-) restricted transformation of molecular ozone into more powerful ($HO^{\bullet}$) species [20]. In the presence of zeolites at pH 3.5 (Fig. 6(a)), the rate of PAA disappearance got increased but in a very limited extent quite similar to plain adsorption effect by HZSM-5 particles (less than 5%, not shown). As solution pH elevated to 9.5, however, the oxidation kinetics enhanced remarkably for zeolite-ozone reaction systems as shown in Fig. 6(b). Ozonation process occurs mainly through a combination of the molecular ozone (O_3) and hydroxyl free radical ($HO^{\bullet}$) pathways as can be globally established by Eq. (2), and for this work, the oxidation kinetics of PAA followed a pseudo-first-order trend for which the overall rate

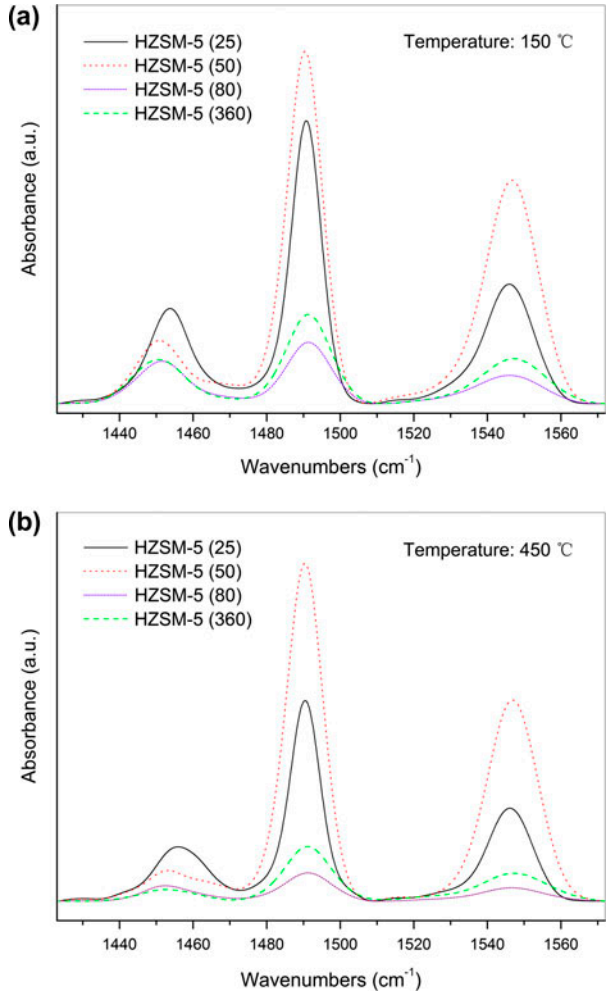

Fig. 4. IR spectra of pyridine adsorbed on HZSM-5 zeolites under (a) 150°C and (b) 450°C.

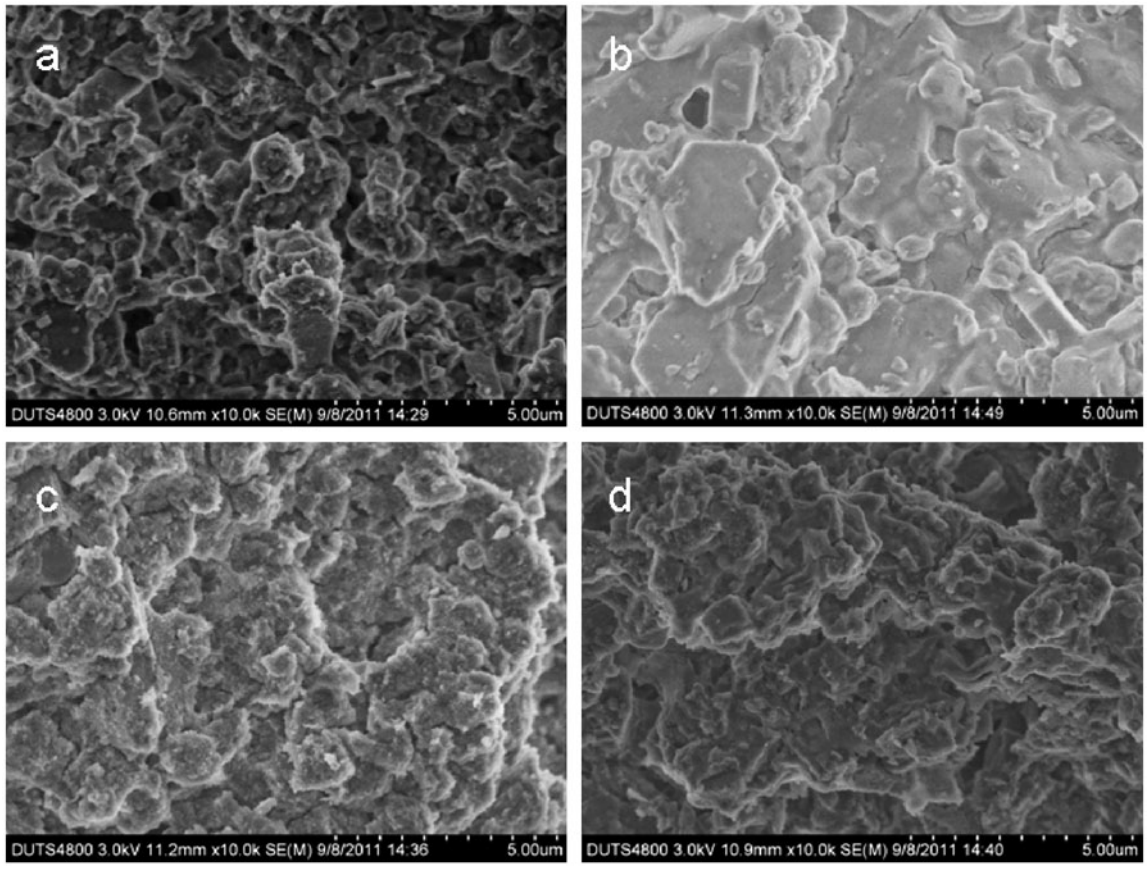

Fig. 5. SEM image of (a) HZSM-5 (25), (b) HZSM-5 (50), (c) HZSM-5 (80), and (d) HZSM-5 (360), respectively.

constants (i.e. the k in Eq. (2)) calculated were listed in Table 2 where R^2 represents the coefficient of determination.

$$-\frac{\mathrm{d}[C]}{\mathrm{d}t} = k_{O_3}[C][O_3]_L + k_{HO\cdot}[C][HO^{\cdot}] \approx k[C] \quad (2)$$

where [C] is the concentration of PAA, t is reaction time, k_{O_3} and k_{HO} are the second-order rate constants, and $[O_3]_L$ and [$HO^{\cdot}$] are the respective concentration of aqueous ozone and hydroxyl radical.

For scenarios under pH 9.5 reading Table 2, HZSM-5 (25) compared to other congeners performed to be more effective on catalytic ozonation of PAA, and the data of kinetics followed HZSM-5 (25) > HZSM-5 (80) > HZSM-5 (360) > HZSM-5 (50), which coincided with the order in amount of Lewis acid sites referring to the total acidity (Fig. 3) and the ratio of Lewis/Brønsted sites (Table 1). Likewise, the abatement of dimensionless TOC that assigned principally to $HO^{\cdot}$ followed the same order as that described for degradation of PAA (see Fig. 7). Results obtained suggested that the presence of HZSM-5 zeolites could have improved the advanced oxidation pathway during ozonation, and this catalytic effect should mainly be subject to the provision of Lewis acid sites.

Further, it is interesting to notice that the degradation profile of PAA was comparable with the addition of HZSM-5 (80) and HZSM-5 (360), and these two zeolites exhibited rather similarity in the amount of weak Lewis acid by analysis on NH_3 desorption curve and IR spectra of adsorbed pyridine at 150°C. This phenomenon indicated that the weak Lewis acid may be more responsible for zeolite-induced catalysis. In fact, the weak Lewis acid sites allow better preservation of hydroxyl groups bonded in the framework structure as Al–OH or Si–OH, which is believed not to be the case for strong Lewis acid that is easy to be deprotonated. And these hydroxyl groups could react with molecular ozone following a way similar to that reported by Staehelin and Hoigné [7]. On the other hand, the weak Lewis acid sites with electro-withdrawing nature are sensitive to capture the free

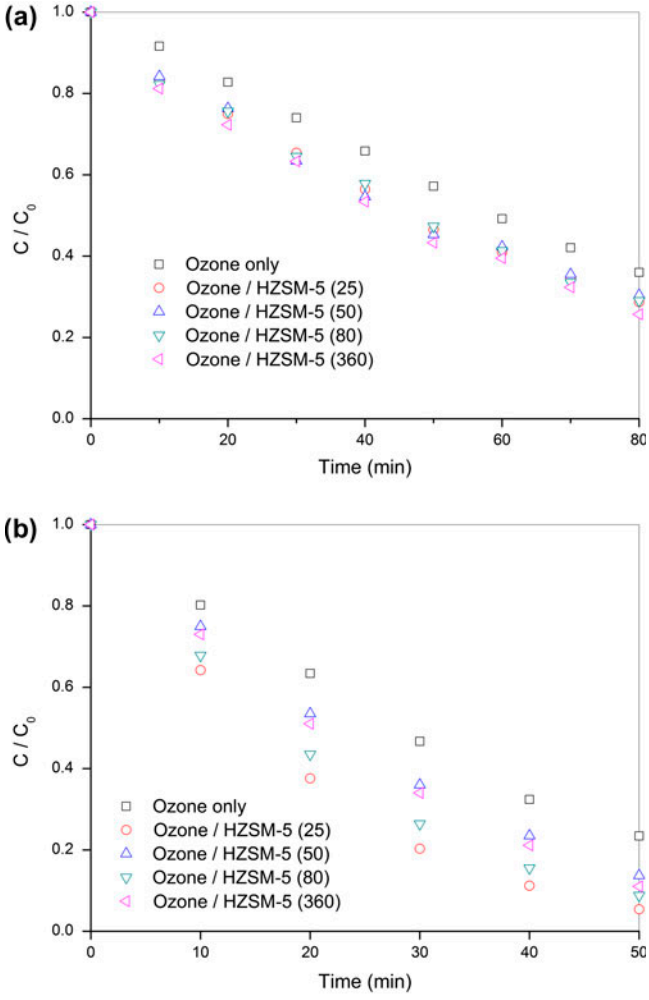

Fig. 6. Evolution of dimensionless concentration of PAA during ozonation with and without HZSM-5 zeolite at (a) pH 3.5 and (b) pH 9.5.

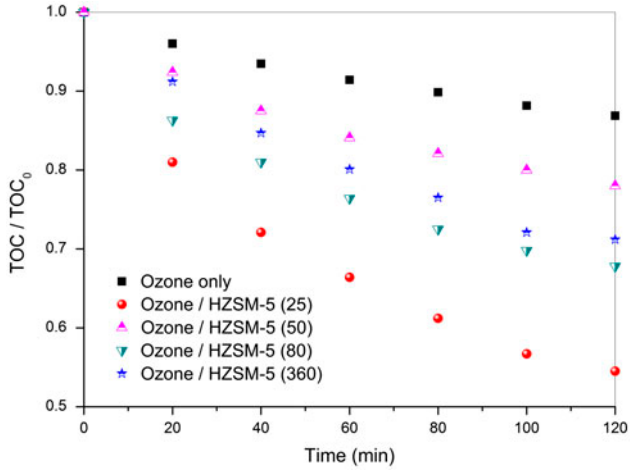

Fig. 7. The remaining TOC at pH 9.5 during ozonation with and without HZSM-5 zeolite.

hydroxyl anions under basic environments, allowing the conjugation of hydroxyl groups on extra-framework aluminum (or more accurately aluminum oxyhydroxides) at zeolitic surface. Consequently, the OH-groups being pre-concentrated on zeolite surface would be fast consumed by aqueous O_3 (adsorbed or diffused), generating locally numerous active ($HO^{\cdot}$) species which in turn led to the reduction of organic loading. As a consequence of analysis and refer to some literatures [7,27], the possible steps delineating the mechanistic processes of catalysis played by HZSM-5 zeolite in progress of ozonation may follow Reactions (3)–(7).

$$L^{*} + H_2O\ (OH^{-}) \rightarrow L^{*}\cdots OH^{-} + H^{+} \quad (3)$$

$$O_3 + L^{*}\cdots OH^{-} \rightarrow L^{*}\cdots HO_2^{-} + O_2 \quad (4)$$

$$O_3 + L^{*}\cdots HO_2^{-} \rightarrow L^{*} + HO^{\cdot} + {}^{\cdot}O_2{}^{-} + O_2 \quad (5)$$

$$O_3 + {}^{\cdot}O_2{}^{-} \rightarrow {}^{\cdot}O_3{}^{-} + O_2 \quad (6)$$

$$O_3 + H_2O \rightarrow HO^{\cdot} + OH^{-} + O_2 \quad (7)$$

where L^{*} represents the active Lewis acid sites dictating catalysis.

Table 2
Pseudo-first-order rate constants for ozonation of PAA with/without HZSM-5 zeolite

	pH 3.5		pH 9.5	
Condition	k ($\times 10^{-2}$ min^{-1})	R^2	k ($\times 10^{-2}$ min^{-1})	R^2
Plain ozonation	1.29	0.990	2.94	0.986
Ozone/HZSM-5 (25)	1.53	0.997	5.64	0.994
Ozone/HZSM-5 (50)	1.48	0.996	3.91	0.992
Ozone/HZSM-5 (80)	1.53	0.994	4.88	0.995
Ozone/HZSM-5 (360)	1.63	0.994	4.56	0.986

In light of these chain reactions, the transformation of dissolved ozone into ($HO^{\bullet}$) products could be largely accelerated in the presence of HZSM-5 zeolites, and for higher solution pH (i.e. pH 9.5), the effect of zeolite exhibited to be much more pronounced on degradation of PAA compared to that under pH 3.5, due to a fast zeolite-surface concentration (Reaction (3)) and *in situ* consumption of hydroxyl ions (HO^{-}) being the initiator for zeolite-induced catalysis (see Reaction (4)).

The concentration of gaseous ozone was online monitored during reaction, and the net absorption rate of ozone determined according to Eq. (1) is shown in Fig. 8. One can see that the presence of HZSM-5 (25) at pH 9.5 substantially accelerated ozone absorption compared to that in the case of ozonation alone, for the corresponding ozone consumption was nearly doubled at the beginning minutes in ozone/HZSM-5 (25) scenario compared to plain ozonation. A more rational explanation may be that HZSM-5 (25) chemically sped up the transformation of dissolved ozone molecules into ($HO^{\bullet}$) species that interacts very fast with parent molecules or intermediates, and simultaneously this process enhanced interfacial driven force of ozone dissolution which in turn improved superficial gas-to-liquid mass transfer (i.e. absorption of ozone). Upon the total disappearance of PAA at about 60 min, the consumption of gaseous ozone with and without HZSM-5 (25) was almost in the same level, implying that the by-product fragments recalcitrant even against ($HO^{\bullet}$) species began to prevail inhibiting the transformation of dissolved ozone molecule as the source of ($HO^{\bullet}$).

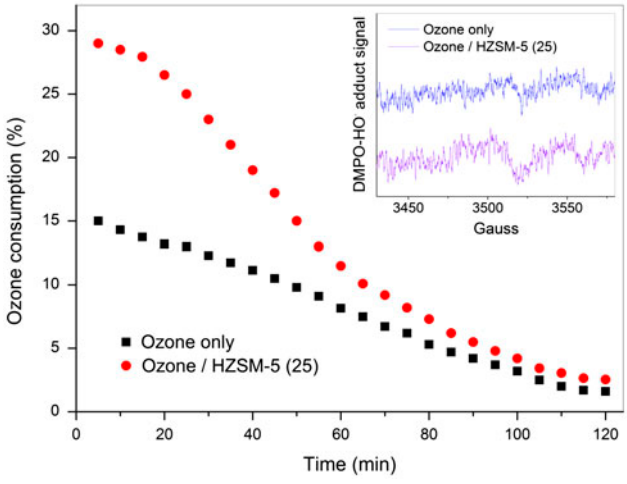

Fig. 8. The profile of ozone consumption rate over time at pH 9.5 (inset: The intensity of DMPO-($HO^{\bullet}$) adduct signal for 10 min ozonation at pH 9.5).

Multiphase catalytic ozonation functionalized by zeolite comprises a combination of reactions in homogeneous and heterogeneous phases. In liquid bulk actually, terminative production of CO_2 would accumulate as a result of mineralization, existing partly in inorganic form of HCO_3^- and CO_3^{2-} that are known to be the scavengers of short-lived ($HO^{\bullet}$) [8]. For this reason, it is usually very hard for the ($HO^{\bullet}$)-pathway to take place in bulk phase as a contribution to degradation of organic contaminants. It can been seen from the inset of Fig. 8 that in both ozone and ozone/HZSM-5 (25) cases at pH 9.5, there was no pronounced DMPO-($HO^{\bullet}$) adduct signal assigned to ($HO^{\bullet}$) species in liquid bulk after 10 min reaction. In the presence of zeolite fortunately, the promotion of ($HO^{\bullet}$) yielding could be accomplished on Lewis acid sites (see Reactions (3)–(7)) and then quickly consumed by organics concentrated in the vicinity or neighborhood of material surface, leading to an evident intensification on degradation of PAA or even mineralization.

In general, HZSM-5 zeolite performed to promote the process of advanced oxidation during ozonation at basic solution, for which the weak Lewis acid sites on zeolitic surface may be principally responsible for the formation of ($HO^{\bullet}$) and its local consumption by organic contaminant. This process inferred is completely different with gas-phase reaction where Brønsted acid was reported playing a key role to remove various volatile organic compounds (VOCs) [28,29]. Incidentally, higher dosage of zeolite is stoichiometrically beneficial to enhance both degradation and mineralization of organic load, the outcome of which is not presented in this study because it is out of scope of current research.

Aluminum leaching is an important issue for utilization of zeolite, since release of aluminum cation (Al^{3+}) will lead to a collapse of extra-framework structure, change material surface property, and even cause severe secondary contamination once overdosed. Yet the elution of Al^{3+} for zeolite-ozone system has seldom been reported by far. As ozonation of PAA progressed, the concentration profile of Al^{3+} over time was recorded and results are shown by Fig. 9. At pH 3.5 where the catalytic effect of zeolite largely suppressed, the Al^{3+} was fast eluted up to concentrations of mg L^{-1} level, possibly due to the frequent cleavage of Al–O bonds by dissociative hydrogen ions (H^+) at acidic solution. At pH 9.5 where HZSM-5 zeolite appreciably works as ozone catalyst, in contrast, the Al^{3+} concentration could be well controlled at rather low level (less than 130 μg L^{-1}) as time prolonged within the covered range of experiments. Hence, basic pH environment is suggested in this work for adoption of zeolite in

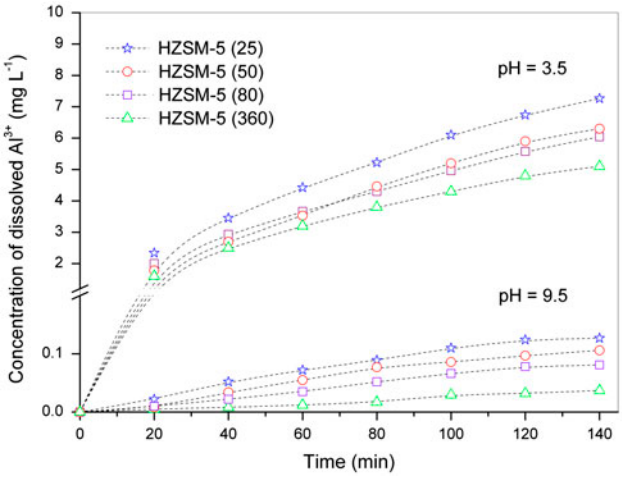

Fig. 9. Dissolved aluminum ion (Al^{3+}) concentration over time in the presence of HZSM-5 zeolite during ozonation of PAA.

assistance to ozonation both for an expected efficiency of catalysis and material stability.

4. Conclusions

Zeolite is surface sensitive mineral that is abundant on earth and naturally available, and extraction of its application possibility for environmental purpose is believed to be of great interest. We tried to combine zeolite with ozone technology in this work for process intensification of advanced oxidation. Generally, utilization of zeolite for catalytic ozonation was proved to be feasible which has been analyzed depending on surface acidity and solution pH. It was suggested that the Lewis acidity under basic pH mainly contributes to the catalytic effect of zeolite, for which it was assumed that both the hydroxyl groups and anions concentrated on the weak Lewis sites had transformed molecular ozone into $HO^{\bullet}$, inducing locally a fast degradation of organic contaminants or even mineralization. Moreover, the framework of zeolite presented to be much more stable at pH 9.5 taking leaching of aluminum ion as reference, which is supportive information for implementation of ozone-zeolite system that better works under basic environments.

Acknowledgements

This work was financially supported by National Basic Research Program of China (No. 2011CB936002), National Science and Technology Major Project (No. 2012ZX07308–002), Natural Science Foundation of Tianjin (No. 12JCYBJC14800), and National Natural Science Foundation of China (No. 51108298).

References

[1] Y. Hu, N. Milne, S. Gray, G. Morris, W. Jin, M. Duke, B. Zhu, Combined TiO_2 membrane filtration and ozonation for efficient water treatment to enhance the reuse of wastewater, Desalin. Water Treat. 34 (2011) 57–62.
[2] J. Rivera-Utrilla, J. Méndez-Díaz, M. Sánchez-Polo, M.A. Ferro-García, I. Bautista-Toledo, Removal of the surfactant sodium dodecylbenzenesulphonate from water by simultaneous use of ozone and powdered activated carbon: Comparison with systems based on O_3 and O_3/H_2O_2, Water Res. 40 (2006) 1717–1725.
[3] F. Pan, Y. Luo, J.J. Fan, D.C. Liu, J. Fu, Degradation of disperse blue E-4R in aqueous solution by zero-valent iron/ozone, Clean-Soil Air Water 40 (2012) 422–427.
[4] P.C.C. Faria, J.J.M. Órfão, M.F.R. Pereira, Ozonation of aniline promoted by activated carbon, Chemosphere 67 (2007) 809–815.
[5] K. Turhan, Z. Turgut, Decolorization of direct dye in textile wastewater by ozonization in a semi-batch bubble column reactor, Desalination 242 (2009) 256–263.
[6] F.J. Beltrán, J.F. García-Araya, I. Giráldez, Gallic acid water ozonation using activated carbon, Appl. Catal. B 63 (2006) 249–259.
[7] J. Staehelin, J. Hoigné, Decomposition of ozone in water: Rate of initiation by hydroxide ions and hydrogen peroxide, Environ. Sci. Technol. 16 (1982) 676–681.
[8] J. Ma, N.J.D. Graham, Degradation of atrazine by manganese-catalysed ozonation-influence of radical scavengers, Water Res. 34 (2000) 3822–3828.
[9] A. Georgi, F.D. Kopinke, Interaction of adsorption and catalytic reactions in water decontamination processes: Part I. Oxidation of organic contaminants with hydrogen peroxide catalyzed by activated carbon, Appl. Catal. B 58 (2005) 9–18.
[10] M. Leili, G. Moussavi, K. Naddafi, Degradation and mineralization of furfural in aqueous solutions using heterogeneous catalytic ozonation, Desalin. Water Treat. 51 (2013) 6789–6797.
[11] J.H.J. Kluytmans, B.G.M. van Wachem, B.F.M. Kuster, J.C. Schouten, Mass transfer in sparged and stirred reactors: Influence of carbon particles and electrolyte, Chem. Eng. Sci. 58 (2003) 4719–4728.
[12] H. Valdés, V.J. Farfán, J.A. Manoli, C.A. Zaror, Catalytic ozone aqueous decomposition promoted by natural zeolite and volcanic sand, J. Hazard. Mater. 165 (2009) 915–922.
[13] H. Valdés, R.F. Tardón, C.A. Zaror, Effect of Zeolite chemical surface properties on catalytic ozonation of methylene blue contaminated waters, Ozone Sci. Eng. 32 (2010) 344–348.
[14] H. Valdés, R.F. Tardón, C.A. Zaror, Role of surface hydroxyl groups of acid-treated natural zeolite on the heterogeneous catalytic ozonation of methylene blue contaminated waters, Chem. Eng. J. 211–212 (2012) 388–395.
[15] A. Ikhlaq, D.R. Brown, B. Kasprzyk-Hordern, Mechanisms of catalytic ozonation: An investigation into superoxide ion radical and hydrogen peroxide formation during catalytic ozonation on alumina and zeolites in water, Appl. Catal. B 129 (2013) 437–449.
[16] J. Rivera-Utrilla, M. Sánchez-Polo, M.I. Bautista-Toledo, J.D. Méndez-Díaz, Enhanced oxidation of sodium dodecylbenzenesulfonate aqueous solution

using ozonation catalyzed by base treated zeolite, Chem. Eng. J. 180 (2012) 204–209.
[17] N.A.S. Amin, J. Akhtar, H.K. Rai, Screening of combined zeolite-ozone system for phenol and COD removal, Chem. Eng. J. 158 (2010) 520–527.
[18] Y. Dong, H. Yang, K. He, X. Wu, A. Zhang, Catalytic activity and stability of *Y* zeolite for phenol degradation in the presence of ozone, Appl. Catal. B 82 (2008) 163–168.
[19] N. Sano, T. Yamamoto, D. Yamamoto, S.I. Kim, A. Eiad-Ua, H. Shinomiya, M. Nakaiwa, Degradation of aqueous phenol by simultaneous use of ozone with silica-gel and zeolite, Chem. Eng. Process. 46 (2007) 513–519.
[20] S. Zhang, D. Wang, S.S. Zhang, X.W. Zhang, P.P. Fan, Ozonation and carbon-assisted ozonation of methylene blue as model compound: Effect of solution pH, Proc. Environ. Sci. 18 (2013) 493–502.
[21] S. Zhang, D. Wang, X. Quan, L. Zhou, X.W. Zhang, Multi-walled carbon nanotubes immobilized on zero-valent iron plates (Fe^0-CNTs) for catalytic ozonation of methylene blue as model compound in a bubbling reactor, Sep. Purif. Technol. 116 (2013) 351–359.
[22] R. Huang, B. Lan, Z. Chen, H. Yan, Q. Zhang, J. Bing, L. Li, Catalytic ozonation of p-chlorobenzoic acid over MCM-41 and Fe loaded MCM-41, Chem. Eng. J. 180 (2012) 19–24.
[23] W.L. Wang, B.J. Liu, X.J. Zeng, Catalytic cracking of C_4 hydrocarbons on ZSM-5 molecular sieves with low SiO_2/Al_2O_3 molar ratio, Acta Phys. Chim. Sin. 24 (2008) 2102–2107.
[24] R. Anand, B.S. Rao, Conversion of piperazine over acidic zeolites, Catal. Commun. 3 (2002) 479–486.
[25] M. Rivera-Garza, M.T. Olguín, I. García-Sosa, D. Alcántara, G. Rodríguez-Fuentes, Silver supported on natural Mexican zeolite as an antibacterial material, Microporous Mesoporous Mater. 39 (2000) 431–444.
[26] R. López-Fonseca, B. de Rivas, J.I. Gutiérrez-Ortiz, A. Aranzabal, J.R. González-Velasco, Enhanced activity of zeolites by chemical dealumination for chlorinated VOC abatement, Appl. Catal. B 41 (2003) 31–42.
[27] R.E. Bühler, J. Staehelin, J. Hoigné, Ozone decomposition in water studied by pulse radiolysis. 1. HO_2/O_2^- and HO_3/O_3^- as intermediates, J. Phys. Chem. 88 (1984) 2560–2564.
[28] D.J. Wylie, R.P. Cooney, J.M. Seakins, G.J. Millar, Spectroscopic studies of the adsorption and reactions of chlorofluorocarbons (CFC-11 and CFC-12) and hydrochlorofluorocarbon (HCFC-22) on oxide surfaces, Vib. Spectrosc. 9 (1995) 245–256.
[29] L. Storaro, R. Ganzerla, M. Lenarda, R. Zanoni, A. Jiménez-López, P. Olivera-Pastor, E. Rodríguez-Castellón, Catalytic behavior of chromia and chromium-doped alumina pillared clay materials for the vapor phase deep oxidation of chlorinated hydrocarbons, J. Mol. Catal. A Chem. 115 (1997) 329–338.